

# Simulated Turn-Off of 4H-SiC Gate Turn-Off Thyristors with Gate Electrodes on the p-Base or the n-Base

Pankaj B. Shah and Kenneth A. Jones

**Abstract**— Turn-off simulations of a 4H-SiC GTO thyristor structure having a gated p-base and p-type substrate are compared with that having a gated n-base and n-type substrate. Two gate drive circuits are considered, one with a voltage source and resistor between the gate and adjacent emitter region, and the other with a voltage source and resistor between the gate and farthest emitter region. The gated n-base thyristor's substrate current increases atypically before the device turns off. Also, the gated n-base structure turns off when the gate circuit is connected directly to the emitter region furthest from the gate region, but the gated p-base structure does not. Furthermore, turn-off gain is lower for the gated n-base structure due to mobility differences as demonstrated by current-voltage ( $I$ - $V$ ) and current versus time ( $I$ - $t$ ) curves.

**Index Terms**—Power conditioning, switching transients, thyristors.

## I. INTRODUCTION

THE 4H-silicon carbide's (SiC) large breakdown electric fields, high-saturation drift velocity, and high thermal conductivity are excellent for fast, high-power switching devices, and the reason for the intense research in developing SiC gate-turn-off (GTO) thyristors [1]–[3]. The slow development of these devices is due in part to poor material quality and the lack of well developed processing techniques, but also due to the device configuration, such as placing the gate contact on the n-type base region. Gate contact placement is dictated by the desire to have an n-type substrate which encourages the use of an n-gated base to avoid the challenging deep etch to the p-base region. N-type substrates are desired because they are cheaper and easier to produce and have traits important for vertical power devices, such as very high free carrier concentrations and low resistance. The GTO thyristor is a current controlled device, and when the gates are on the n-base, current control of the anode-cathode current by the gate current is a challenging design problem. In this letter, we indicate the best gate drive circuit connection, and demonstrate that the design and circuit configurations are as important considerations as material quality.

Manuscript received January 13, 1999; revised July 7, 1999. This work was performed while P. Shah was a National Research Council Associate at the Army Research Laboratory.

The authors are with the U.S. Army Research Laboratory AMSRL-SE-RL, Adelphi, MD 20783 USA (e-mail: pshah@arl.mil).

Publisher Item Identifier S 0741-3106(99)08741-8.

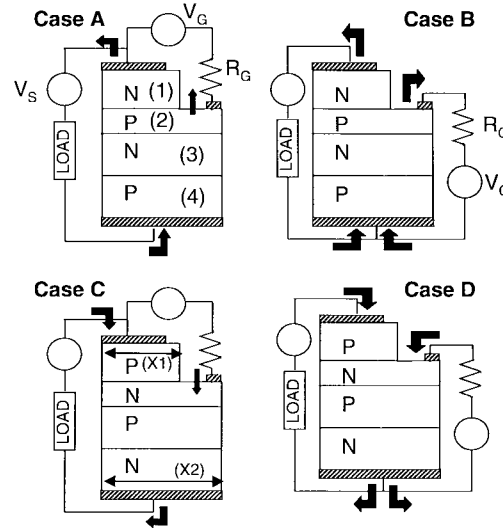


Fig. 1. Diagrams showing the four cases considered in this paper. The dopant concentrations for the different regions are 1)  $1 \times 10^{18} \text{ cm}^{-3}$ , 2)  $3 \times 10^{17} \text{ cm}^{-3}$ , 3)  $1 \times 10^{17} \text{ cm}^{-3}$ , and 4)  $1 \times 10^{18} \text{ cm}^{-3}$ . N and P indicate that the dopants are donors or acceptors respectively. The striped areas are electrical contacts. Regions 1–4 are sequentially the same in all four cases, and the gate contact is the striped area touching region 2.  $X1 = 11 \mu\text{m}$ , and  $X2 = 14 \mu\text{m}$ . The thick arrows indicate the direction of current flow when the turn-off process begins. The thickness of regions 1, 2, 3, and 4 are 3, 1.65, 6.5, and  $5.85 \mu\text{m}$ , respectively.

## II. MODEL

Mixed-mode two-dimensional drift-diffusion model numerical-simulations were done using Atlas/Blaze [4] for the cases presented in Fig. 1. Dopant concentrations for the layers numbered in Fig. 1 (case A) are: 1)  $1 \times 10^{18} \text{ cm}^{-3}$ , 2)  $3 \times 10^{17} \text{ cm}^{-3}$ , 3)  $1 \times 10^{17} \text{ cm}^{-3}$ , and 4)  $1 \times 10^{18} \text{ cm}^{-3}$ . These values are the same for the respective layer in all four cases, being donors in n-type regions and acceptors in p-type regions (the layer with the gate is doped  $3 \times 10^{17} \text{ cm}^{-3}$  whether the dopants are donors or acceptors). Cases A and B are gated p-base structures, and Cases C and D are gated n-base structures. The load circuit consists of a current source in parallel with a  $2 \text{ k}\Omega$  resistor and the gate drive circuit consists of a voltage source in series with a resistor.

The material characteristics are included as follows. The energy gap is  $3.21 \text{ eV}$ , the electron effective density of states is  $1.66 \times 10^{19} \text{ cm}^{-3}$ , the hole effective density of states is  $3.286 \times 10^{19} \text{ cm}^{-3}$ , the relative permittivity of SiC is 10, the donor ionization energy is  $65 \text{ meV}$ , and the acceptor ionization

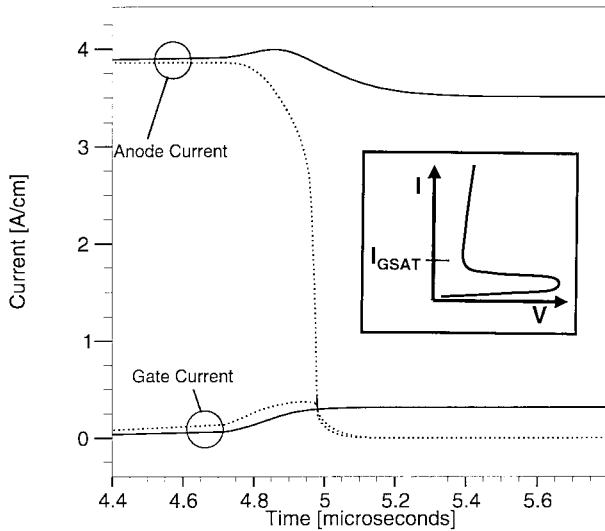


Fig. 2. Transient turn-off curves for gated p-base structures and gate drive circuits of case A (dotted curve) and B (solid curve), showing magnitude of substrate electrode (anode) current and gate current: Inset shows example of steady-state  $I-V$  curve and indicates how  $I_{GSAT}$  is defined.

energy is 191 meV. Selberherr band gap narrowing model for silicon is used [5]. Auger recombination coefficients are  $C_n = 5 \times 10^{-29} \text{ cm}^6/\text{s}$  and  $C_p = 9.9 \times 10^{-32} \text{ cm}^6/\text{s}$  [5]. The  $C_n$  value used here is slightly higher than the values reported [6], [7]. Measured impact ionization data [8] for the ionization rate,  $\alpha_{n,p}$  is included with the following model:

$$\alpha_{n,p} = a_{n,p} \exp \left[ -\frac{b_{n,p}}{E} \right]$$

where for electrons in low-field regions  $a = 2.1 \times 10^7 \text{ cm}^{-1}$ , and  $b = 2.63 \times 10^7 \text{ V cm}^{-1}$ , while for a field greater than  $E_c = 4 \times 10^6 \text{ V cm}^{-1}$ ,  $a = 7.3 \times 10^6 \text{ cm}^{-1}$ , and  $b = 2.15 \times 10^7 \text{ V cm}^{-1}$ . For holes in a low field region,  $a = 7 \times 10^6 \text{ cm}^{-1}$  and  $b = 1.41 \times 10^7 \text{ V cm}^{-1}$  while for a field greater than  $E_c$ ,  $a = 3.5 \times 10^6 \text{ cm}^{-1}$  and  $b = 1.2 \times 10^7 \text{ V cm}^{-1}$ . A field dependent mobility model was used, and for the concentration dependence the electron and hole mobility,  $\mu_n, \mu_p$ , in  $\text{cm}^2/\text{V s}$  for the regions, as numbered in Fig. 1 (case A) are 1) 250:94, 2) 365:103, 3) 560:108, and 4) 250:94. Similarly, the Shockley-Read-Hall lifetimes [9],  $\tau_n, \tau_p$ , in nanoseconds for the regions as numbered in Fig. 1 (case A) are 1) 400:100, 2) 200:50, 3) 2000:500, and 4) 5000:1000. The lower lifetimes in the higher epilayers accounts for their poorer quality. In all the thyristor structures, region 1 is the top region. These models accurately predict the on-state performance and current-voltage ( $I-V$ ) curve negative-differential-resistance region characteristics of previously measured devices [9].

### III. RESULTS AND DISCUSSIONS

Steady-state simulations indicate that the maximum blocking voltage of the GTO thyristor in case A or B is 324 V, while that for the GTO thyristor in case C and D is 228 V. Fig. 2 presents turn-off simulation results for cases A and B. Case A turns off as expected with a resistive load [10] and

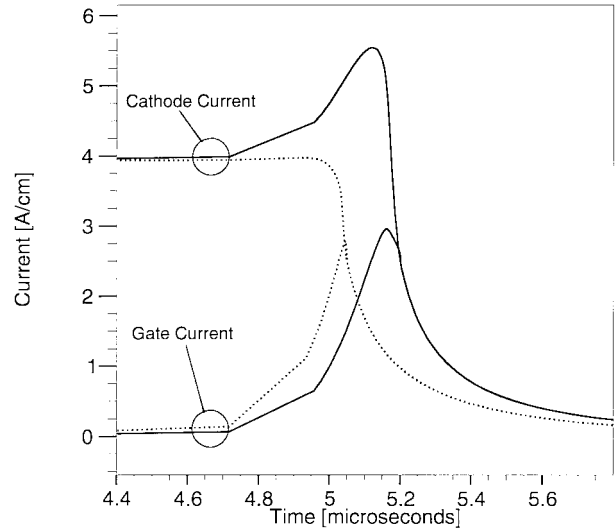


Fig. 3. Transient turn-off curves for gated n-base structure and gate drive circuits of case C (dotted curve) and D (solid curve), showing magnitude of substrate electrode (cathode) current and gate current.

has a turn-off gain  $\beta_{\text{off}} \sim 8$ .  $\beta_{\text{off}}$  [11], is the ratio of the substrate current turned off to the gate current causing the turn-off. Case B doesn't turn off as the gate circuit resistance is reduced indicating that the thyristor limits the gate current. Fig. 3 presents the turn-off performance for cases C and D. During turn-off of case C, the current flowing through the load increases slightly (from 3.92 to 3.97 A/cm) and then the device turns off with  $\beta_{\text{off}} \sim 1.3$ . Case D has a larger  $\beta_{\text{off}} \sim 2$  and a strong substrate current increase during turn-off. In other not as optimal structures the gate current increased substantially above the initial cathode current before the device turned off.

Both the turn-off mechanism and how the gate drive circuit influences it explain these differences. The gate drive circuit affects the current flow at the thyristor's contacts. Simulations indicated that for cases A and C as the gate current increased, the top electrode current decreased, while for cases B and D as the gate current increased, the bottom electrode current increased. To understand this, follow the thick current flow arrows in Fig. 1 and take into account the contact regions' majority carrier concentrations and mobilities. (The current flowing into the device from the bottom electrode in case A, flows out through both the top and the gate electrode.) For case C, the majority carrier electrons in the lower emitter region have higher mobility so the strong gate current was also partially supplied by an increase in the lower electrode current. The increasing substrate electrode current of case C presents a threat to the load but for case D the increase in the substrate current only affected the gate drive circuit. The maximum gate current during turn-off is slightly higher at 2.96 A/cm for case D compared to 2.79 A/cm for case C.

GTO thyristor turn-off is initiated when majority carriers are removed from the base region through the gate contact. The device then maintains an on-state with fewer carriers and a larger bias across the device as the remaining carriers squeeze away from the gate electrode to form a narrow current channel. The extracted concentration and the carrier mobility play a crucial role here. As the turn-off mechanism proceeds

for case B the anode-cathode current is squeezed away from the gates and the holes that should be extracted are deep in the p region. This hole extraction current must flow through the highly resistive gate vicinity. Case D doesn't exhibit this problem because fewer electrons are extracted for a given amount of current so that the gate vicinity is not as highly depleted, and the gate drive can extract a sufficient amount of carriers further from the gate contact.

Another steady-state indicator of thyristor switching performance is the ratio of the current where the bias increases for decreasing current,  $I_{GSAT}$  (see inset of Fig. 2), to the gate current  $I_G$ . It should be large, indicating that carriers contributing to the injection efficiency at the emitter-base junction to maintain the thyristor action are instead extracted through the gate. With  $I_G = 0.4$  A/cm,  $I_{GSAT}/I_G$  is larger for the gated p-base structure ( $5.15/0.4 = 12.87$ ) compared to the gated n-base structure ( $0.825/0.4 = 1.83$ ). The gated p-base structure has this ratio and  $\beta_{off}$  both larger because holes have lower mobility so to produce a given gate current, more holes are removed than the number of electrons to be removed in a gated n-base structure with the same gate current. However, the ratio increases with gate current for the gated n-base structure (when  $I_G = 3$  A/cm,  $I_{GSAT}/I_G = 8.75/3 = 2.916$ .) Turn-off gain increases at higher current because the higher current is due to more free carriers rather than increased mobility. Therefore, a larger gate current extracts a proportionately larger carrier concentration from the base region.

#### IV. CONCLUSION

Turn-off simulations of the gated p-base and gated n-base 4H-SiC GTO thyristors with similar doping profiles have been presented. We compare connecting the gate drive circuit between the gated base and the nearest emitter region to connecting the gate drive circuit between the gated base and

the furthest emitter region. Results indicate that the load current may increase during turn-off of gated n-base thyristors. In some cases during turn-off the gate and substrate currents are higher than the initial substrate current, making device failure more likely. The gated p-base structure did not turn off when the gate was connected to the furthest emitter region. The gated n-base thyristor's lower turn-off gain is attributed to fewer majority carriers removed from the gated base region for a given gate current compared to the gated p-base structure.

#### REFERENCES

- [1] A. K. Agarwal, J. B. Casady, L. B. Rowland, S. Seshadri, R. R. Siergiej, W. F. Valek, and C. D. Brandt, "700-V asymmetrical 4H-SiC gate turn-off thyristors (GTO's)," *IEEE Electron Device Lett.*, vol. 18, p. 518, 1997.
- [2] K. Xie, J. H. Zhao, J. R. Flemish, T. Burke, W. R. Buchwald, G. Lorenzo, and H. Singh, "A high-current and high-temperature 6H-SiC thyristor," *IEEE Electron Device Lett.*, vol. 17, p. 142, 1996.
- [3] M. E. Levinshstein, J. W. Palmour, S. L. Rumyanetsev, and R. Singh, "The critical charge density of 4H-SiC thyristors," *IEEE Trans. Electron Devices*, vol. 45, p. 307, 1998.
- [4] *Atlas User's Manual*, Silvaco International, 1997.
- [5] S. Selberherr, *Analysis and Simulation of Semiconductor Devices*. Vienna, Austria: Springer-Verlag, 1984.
- [6] A. Galeckas, J. Linnros, V. Grivickas, U. Lindefelt, and C. Hallin, "Evaluation of auger recombination rate in 4H-SiC," *Mater. Sci. Forum*, vol. 264-268, p. 533, 1998.
- [7] N. Ramungul, V. Khemka, T. P. Chow, M. Ghezzi, and J. Kretschmer, "Carrier lifetime extraction from a 6H-SiC high voltage p-i-n rectifier reverse recovery waveform," *Mater. Sci. Forum*, vol. 264-268, p. 1065, 1998.
- [8] A. O. Konstantinov, Q. Wahab, N. Nordell, and U. Lindefelt, "Ionization rates and critical fields in 4H silicon carbide," *Appl. Phys. Lett.*, vol. 71, p. 90, 1997.
- [9] P. B. Shah and K. A. Jones, "Two-dimensional numerical investigation of the impact of material-parameter uncertainty on the steady-state performance of passivated 4H-SiC thyristors," *J. Appl. Phys.*, vol. 84, p. 4625, 1998.
- [10] A. Nakagawa and D. H. Navon, "A time- and temperature-dependent 2-D simulation of the GTO thyristor turn-off process," *IEEE Trans. Electron Devices*, vol. ED-31, p. 1156, 1984.
- [11] S. M. Sze, *Physics of Semiconductor Devices*, 2nd ed. New York: Wiley, 1981.